Adsorption of Sodium Dodecyl Sulfate at Water-Dodecane Interface in Relation to the Oil in Water Emulsion Properties

Adsorption of SDS at water/dodecane interface in relation to the oil in water emulsion properties

Journal:	*Langmuir*
Manuscript ID	la-2018-00358g.R1
Manuscript Type:	Article
Date Submitted by the Author:	30-Mar-2018
Complete List of Authors:	Llamas, Sara; CNR-Institute of Condensed Matter Chemistry and technologies for Energy, Unit of Genoa Santini, Eva; CNR-Institute of Condensed Matter Chemistry and Technologies for Energy, Unit of Genoa Liggieri, Libero; CNR-Institute of Condensed Matter Chemistry and Technologies for Energy, Unit of Genoa Salerni, Fabrizia; University of Parma Orsi, Davide; University of Parma, Department of Mathematical, Physical and Computer Science Cristofolini, Luigi; University of Parma, , Department of Mathematical, Physical and Computer Science Ravera, Francesca; CNR-Institute of Condensed Matter Chemistry and Technologies for Energy, Unit of Genoa

Adsorption of SDS at water/dodecane interface in relation to the oil in water emulsion properties

Sara Llamas,[1] Eva Santini,[1] Libero Liggieri,[1] Fabrizia Salerni,[2] Davide Orsi,[2] Luigi Cristofolini,[1,2] Francesca Ravera[1,*]

[1]*CNR-Institute of Condensed Matter Chemistry and Technologies for Energy, Via de Marini 6, 16149 Genoa, Italy*

[2]*Department of Mathematical, Physical and Computer Sciences, University of Parma, Viale Usberti 7 A, 43124 Parma, Italy*

** Corresponding author: francesca.ravera@ge.icmate.cnr.it*

Abstract

The control of the behavior of oil in water emulsions requires deepen investigations on the adsorption properties of the emulsion stabilizers at interfaces, being these fundamental to explain the (de)stabilization mechanisms.

In this work, we present an extensive study on oil-in-water emulsions stabilized by Sodium Dodecyl Sulfate (SDS) below its critical micellar concentration. Dynamic tensiometry, dilational rheology and electrical conductivity measurements are used to investigate the adsorption properties at the droplet interface, while the ageing of the respective emulsions was investigated by monitoring the macroscopic thickness of the emulsion layer, by micro-imaging and Dynamic Light Scattering (DLS) analysis, to get information on the drop size distribution. In addition, the droplet coalescence is investigated by a microscopy set-up.

The results of this multi-techniques study allow deriving a coherent scenario where the adsorption properties of this ionic surfactant relate to those of the emulsion, such as for example, the prevention of droplet coalescence and the presence of other mechanisms, such as Ostwald ripening, responsible of the emulsion ageing.

Keywords: adsorption isotherm; emulsion stability; ionic surfactants; Ostwald ripening; coalescence; droplet size distribution

Introduction

Emulsions are colloidal systems interesting for a wide range of industries: chemical, pharmaceutical, cosmetic or food among others [1, 2, 3, 4, 5]. The control of lifetime of emulsions is essential for all those technological applications. Different emulsifiers can be used to stabilize emulsions by modifying the liquid-liquid interface properties. Hence, the adsorption of surfactants, polymers, proteins or nanoparticles to the interface plays an essential role in the creation and stability of the emulsions [6,7,8, 9,10].

The adsorption of surfactants, in fact, reducing the interfacial tension and, as a consequence, the surface free energy of the liquid-liquid system, favors the creation of larger interfacial area during the emulsification process.

The main processes involved in the evolution of emulsions, are creaming or sedimentation – the gravity driven phase separation due to density differences -, Ostwald ripening and coalescence [8,11,12]. Ostwald ripening consists in the transfer of molecules of the dispersed liquid phase from small to large droplets. This phenomenon is driven by the difference of Laplace pressure of the droplets, which is inversely proportional to the radius, and reflects in a net mass transfer from small to big droplets [13,14]. The presence of adsorbed surfactant, inducing a dilational elastic character to the interface, may have the effect of hindering or, in some case, arresting the solvation of droplets [15]. This effect is quantified by the Gibbs criterion [16], which asserts that the drop size evolution stops when the dilational elasticity overcomes half the value of the interfacial tension. Coalescence is the process in which two emulsion droplets merge into a single larger one, due to the rupture of the liquid film between them. The thinning of this liquid film, which can lead directly to its rupture or to the formation of a thin common black film (10-100 nm), is a complex hydrodynamic process mainly driven by the mechanical properties of the water-oil interfaces, such as dynamic interfacial tension and dilational viscoelasticity [17, 18, 19]. High elasticity, for example tends to hinder this thinning, making more stable the liquid films. From this, it follows the importance to investigate the adsorption properties of emulsion stabilizer surfactants. Moreover, the behavior of thin films, mainly governed by disjoining pressure, also depends on large extend on the adsorption properties of

surfactants [20], which can be accessed by dynamic and equilibrium interfacial tension investigation.

Reducing the amounts of surfactant is a valuable target for emulsion technology. To this aim it is very important to assess the emulsion properties below the critical micellar concentration (cmc) of the surfactant. In this regime, interfacial properties and their impact of the destabilization processes vary significantly with surfactant concentration.

In this work, we chose to investigate dodecane-in-water emulsions stabilized by Sodium Dodecyl Sulfate (SDS) in the range of concentration below the cmc. SDS is one of the most used ionic surfactant employed in a wide number of applications. In particular, SDS has been largely investigated at water/dodecane interface [21, 22] as well as stabilizer for dodecane-in-water emulsions [13, 23, 24, 25]. The reason for this propensity to use dodecane, as oil phase with SDS is that, among the impurities contained in SDS, one of the most critical is dodecanol, produced by spontaneous hydrolisis. Due to its high surface activity, in fact, dodecanol plays a dominant effect in the adsorption to the interface with respect to SDS, even when present in trace amounts [26, 27]. However, in water/dodecane systems, because of its large solubility in dodecane, dodecanol is transferred into the oil phase, without affecting the adsorption of SDS.

In this paper, we present an extensive study of this system, carried out characterizing the liquid-liquid interfacial properties, by interfacial tension and dilational rheology measurements, and the behavior of the respective emulsions, by monitoring the macroscopic thickness of the emulsion layer and by microscope observation and Dynamic Light Scattering (DLS) analysis to obtain information on the droplet size distribution.

Moreover, electrical conductivity measurements have been carried out to estimate the surfactant depletion of the aqueous phase induced by the huge increase of the interfacial area during emulsification. This effect is recognized to be very important to better understand the relation between interfacial properties and stability of disperse system. Both for foams [28] and in case of emulsions [29,30]. Moreover, the evaluation of the actual concentration of the aqueous phase carried out in this study, allows estimating the total interfacial area created by emulsification.

Finally, to complement this multi-techniques experimental study, using a purposely-designed device, we investigated the behavior of two interacting bubbles to find the coalescence conditions.

Experimental Section

Materials

Dodecane and Sodium dodecyl sulfate (SDS) were purchased from Sigma-Aldrich (Germany) with purity higher than 99% and used without further purification. The water used were produced by a Millipore (Elix + Milli-Q) purification system with resistivity higher than 18 MΩ·cm and a stable surface tension of about 72.5 mN/m at 20 °C. The value of the interfacial tension of dodecane against pure water was found 51.3 mN/m, not varying appreciably during one thousand seconds.

All glass materials utilized in the samples preparation and measurements were carefully cleaned with surfuric acid and subsequently rinsed with plentiful Milli-Q water in order to remove any impurity. With the same purpose, any other not glass materials were cleaned with isopropanol and rinsed with Milli-Q water.

Methods

A drop shape tensiometer [31] (PAT1 - Sinterface, Germany) was used for interfacial tension and dilational rheology measurements.

According to this technique, the value of the interfacial tension is obtained as result of a fitting procedure where the Laplace theoretical profile for axisymmetric gravity-deformed drops, under mechanical equilibrium, is fitted to the experimentally acquired profile of a liquid drop or bubble. More details on this technique are reported in ref. 32. For the present study an emerging drop of dodecane, with volume of about 30 mm^3, is formed, in a time of about 1 second, at the tip of a U-shaped capillary tube immersed in aqueous SDS solution. The interfacial tension is acquired while maintaining constant the drop surface area since the formation of a fresh interface to a time long enough to warrant the achievement of the adsorption equilibrium.

Using the same tensiometer, the dilational viscoelasticity, E, versus frequency is obtained by the Oscillating Drop method [31]. Accordingly, after the achievement of the adsorption equilibrium, sinusoidal perturbations of the interfacial area (A) are imposed to the drop,

while the continuous acquisition of the interfacial tension. To obtain the real and imaginary parts of *E* the following expression is used

$$E = \frac{\Delta\gamma}{\Delta A/A_0} e^{i\varphi} \qquad (1)$$

where $\Delta\gamma$ and ΔA are the amplitudes of the oscillating surface tension and surface area, respectively, A_0 the reference area and φ the phase shift between the surface tension and surface area signals. For each frequency, ν, these quantities are extracted by the acquired signals, by using the concepts of Fourier analysis. In this way, the complex dilational viscoelasticity against frequency is evaluated in a range from 0.005 to 0.2 Hz. The upper limit of the frequency range, typical of this technique, is due to the necessity to work under mechanical quasi-equilibrium condition, which is a requirement for the Laplace equation applicability [31]. All measurements reported below have been performed at 20ºC.

Drop coalescence experiments have been performed in a purposely-designed set-up, housed on the stage of an optical microscope. In this apparatus, two liquid droplets are formed at the tip of small stainless steel capillaries, with diameter of 0.4 mm, immersed in a second liquid contained in a cell, with volume of about 18 cm^3. The growth of the droplets is controlled by computer-driven high precision syringes. The system is also equipped by 3-axial mechanical micromanipulators to bring in contact the droplets and, if needed, press them one against the other. The experiments are video-recorded for further analysis by using a USB 1024 x 768 pixels camera mounted on the microscope ocular.

Specifically, in this study, droplets of pure dodecane with typical diameters of 1-2 mm, are investigated immersed in SDS solutions. This configuration corresponds to that of the oil in water emulsions stabilized by SDS.

Emulsions are obtained by mixing the two liquid phases, using an Ultraturax mixer (IKA ULTRA TERPAX T25), at 10.000 rpm for 10 minutes. The volume fractions of dodecane, Φ_d, in the emulsions investigated were 0.2 and 0.5.

Emulsions are produced in glass beakers using a total liquid amount of 20 ml. A portion of the emulsion is immediately transferred to glass vials of 4 ml (15 mm diameter and 48 mm height). The evolution of the dodecane-in-water emulsion is then monitored by measuring

the height of the emulsion phase, h_{em}, during the separation process. The time dependence of the relative emulsion height, $\mathrm{h_r} = \mathrm{h_{em}}/\mathrm{h_t}$, where h_t is the height of the total liquid in the container, provides the first information on the stability of the obtained emulsions.

To monitor the temporal evolution of the average droplet radius, the same emulsions are transferred in appropriate cells to acquire and statistically analyze optical microscope images.

More information on the evolution of the drop sizes in diluted samples were obtained by DLS (Dynamic Light Scattering), by means of a Zetasizer-Nano (Malvern Instrument,UK). By this instrument, the intensity autocorrelation function is obtained using the red line (λ = 632 nm) of a He-Ne in a quasi-backscattering configuration (θ = 173°). The technique is applied here to evaluate the drop size distribution of the emulsions at different degree of destabilization, or time from the emulsification. To fulfill the DLS requirement of single-scattering event, highly diluted samples are required. The droplet size distribution at different ageing times was then evaluated by performing the measurements on emulsion batches with the desired age, diluted by a factor 10 with corresponding SDS solution just before the measurement.

The analysis of the normalized autocorrelation functions of the scattered intensity $g^2(t)$ provides the distribution of apparent diffusion coefficient and, through the Stokes-Einstein relation, the droplet hydrodynamic diameter [33]. The application of this method to evaluate the droplet size requires the condition of purely Brownian motion for the emulsion droplets that, for the systems here investigated, can be satisfied only after a transient phase, when the creaming process is no more relevant, being the larger droplets transferred away from the acquisition zone. The analysis of the autocorrelation functions to obtain the droplet distributions is based on a well-established approach utilizing the CONTIN algorithm [34].

Electrical conductivity measurements have been utilized to estimate the actual bulk concentration of the aqueous phase after the emulsification. This method is based on the direct relation between the electrical conductivity of an ionic surfactant solution and its concentration [35]. For emulsions, due to the surfactant adsorption at the droplet interfaces, this concentration may be different from the initial one

To this aim, the electrical conductivity of the aqueous matrix phase, spilled from the emulsion, is measured using a high-resolution electrode (+Pt 100 5071 for Crison Basic 30 EC conductometer). The actual concentrations of the aqueous matrix phase are then evaluated by comparing these values with a previously determined master curve of the conductivity versus the ionic surfactant concentration.

Results

Interfacial properties

Figure 1 shows the dynamic interfacial tensions measured during the adsorption kinetics at the interface between pure dodecane and SDS aqueous solutions with concentration c, spanning from $1 \cdot 10^{-5}$ to $7 \cdot 10^{-2}$ M. The corresponding equilibrium interfacial tensions are reported in Figure 2. The equilibrium adsorption properties of SDS have been widely investigated at water/air interfaces [36, 37] and some results on SDS adsorption at oil/water interfaces are also found in literature [38, 39]. As in most cases where ionic surfactants are concerned, the theoretical adsorption isotherms used to interpret the equilibrium surface tension of SDS are those assuming an electrostatic interaction among the adsorbed molecules. That is for example the Frumkin isotherm, for which the equilibrium surface pressure $\Pi=\gamma_0-\gamma$, and the bulk surfactant concentration, c, are related through the following equations, in terms of the surface coverage $\theta = \Gamma\omega$,

$$\Pi = -\frac{\mathrm{RT}}{\omega}\left[\ln(1-\theta) + a_F\theta^2\right] \qquad (2)$$

$$\mathrm{bc} = \frac{\theta}{1-\theta}\,\mathrm{e}^{-2a_F\theta} \qquad (3)$$

where b is the adsorption equilibrium constant, a_F the Frumkin interaction parameter, γ_0 the surface tension of the pure solvent, R the gas constant, T the temperature and ω the molar area of the adsorbed surfactant. This latter, in some cases, is assumed to vary with the surface pressure, as $\omega=\omega_0(1-\varepsilon\Pi)$, to account for a 2D compressibility of the adsorbed layer [40].

On the other side, recent studies [41, 42] have shown that at small coverage the alkyl tail of SDS molecules adsorbed at the water-alkane interface can lie parallel to the interface. Such conformation is due to the relatively large occurrence of gauche defects [43] in the alkyl chain, favored by the interaction with the oil molecules. Being free to rotate, under

these conditions SDS molecules project an area of the order of few square nanometers. By increasing the surface coverage – that is, the SDS concentration in the solution – such conformational disorder disappears due to the molecules packing, and the area occupied tends to the saturation limit of the vertically oriented molecules, compatible with the reported literature values of 40-70 $Å^2$. It is worth to stress that such reorientation capability seems a specific feature of SDS at the water-oil interface, resulting from the interaction of the alkyl tail with the alkane, even if, some authors report similar phenomena also for SDS at water-air interface [44].

The features of an adsorbed layer in which the surfactant molecules (or, more often, one of his moieties) re-orient - from the horizontal to the vertical direction - under the effect of the packing are well captured by the two-state adsorption model [45, 46].

According to this model, the surfactant molecules may adsorb at the interface assuming two different areas per mole, ω_1 and ω_2, corresponding, for example, to the parallel and normal orientation of the molecule with respect to the interface. The distribution of the adsorbed molecules between these two states depends on the degree of surface coverage, related to the equilibrium interfacial tension. This model provides the following equilibrium relation between surface pressure, $\Pi=\gamma^0-\gamma$ and total adsorption Γ,

$$\Pi = -\frac{RT}{\omega}\ln(1-\Gamma\omega) \qquad (4)$$

ω is here the average surface molar area weighted by the adsorptions in the two states, Γ_1 and Γ_2, i.e. $\omega=(\omega_1\Gamma_1+\omega_2\Gamma_2)/(\Gamma_1+\Gamma_2)$. Accordingly, the Π-c adsorption isotherm reads

$$bc = \frac{1-e^{-\frac{\Pi\omega}{RT}}}{\left(\frac{\omega_1}{\omega_2}\right)^{\alpha} e^{-\frac{\Pi\omega_1}{RT}}+e^{-\frac{\Pi\omega_2}{RT}}} \qquad (5)$$

where b and α are two parameters related to the surface activity of the two states which, together with ω_1 and ω_2, completely describe the equilibrium adsorption properties of the system.

Such model, though adequate to describe the features of the re-orientation of SDS molecules at the water-oil interface, does not account for the lateral interaction of the ionic surfactants.

In order to evaluate the effect of this interaction, we performed a comparative analysis of the equilibrium interfacial tension data according to the two states model and to an extended Frumkin Isotherm accounting also for a 2D compressibility of the adsorption layer [47].To this aim the theoretical isotherms have been fitted to the experimental data using the ISOFIT package [48].

As shown in Figure 2, the measured equilibrium interfacial tensions are well described by both the theoretical isotherms, the agreement with the two states isotherm being only slightly better. However, the two models provide appreciably different trends of the surface coverage against the bulk concentration (red curve in Figure 2) and of the parameters more related to the dynamic behavior of the systems such as the Gibbs elasticity, $E_{0,}$ and the characteristic frequency of diffusion, ν_D, (Figure 3), defined in the following as rheological parameters. In particular, for the two-state model, the coverage $\omega\Gamma=\omega_1\Gamma_1+\omega_2\Gamma_2$ shows a plateau with values close to saturation already at a concentration of about three orders of magnitude below the cmc.

The best-fit values of the isotherm parameters, reported in Table 1, are coherent with their physical meaning i.e. the occupational area of the SDS molecules and the degree of surface activity of such kind of surfactants at liquid-liquid interfaces [27]. In particular, the two-state model provides values for ω_1 and ω_2, which are in agreement with the occupied molecular areas reported elsewhere [42] for the SDS molecules respectively lying parallel or packed vertically to the interface.

The analysis of the equilibrium interfacial tension versus the SDS concentration also allows evaluating the critical micellar concentration cmc of SDS in water. The value cmc=8.3 10^{-3} M, obtained assuming the two state adsorption model, is in agreement with that available in literature [27] at 20 °C.

Figure 4 reports the dilational viscoelasticity, *E*, against the SDS concentration for frequency spanning in the range 0.005-1 Hz. The behavior exhibits an increase of the *E* modulus up to a maximum, followed by a decrease towards zero while approaching the cmc, that is the classical tendency for common soluble surfactants [49]. For these systems, in fact, the diffusion process re- equilibrating the concentration profile is the main mechanism governing the rheological response. Its characteristic time decreases with the

surfactant concentration. The maximum arises from the interplay between the dilution of the adsorption layer caused by the interface dilatation and the diffusive surfactant exchange between the interface and the adjacent bulk, which tends to re-equilibrate it. During the process the interfacial tension varies with the adsorption, following the isotherm. At low surfactant concentration the diffusion is slow but the variations of interfacial tensions are small, according to the slope of the isotherm. The values of E remain therefore small. Increasing the concentration, the interfacial tension variations increase but the diffusion process is more and more effective in contrasting the dilution of the adsorption layer. Thus at a given perturbation frequency, the IT variation passes through a maximum and tends to vanishes at the highest concentrations.

Figure 5 reports some examples of measured modulus of *E* against the frequency, ν. The fitting curves, also reported in the figure, have been calculated by a rather general theoretical expression of the complex dilational viscoelasticity which takes into account, as governing processes of the adsorption kinetics, both the bulk diffusion and a re-arrangement process occurring within the interfacial layer [50]. This equation reads,

$$\mathrm{E} = \left[\frac{\mathrm{E}_1+\mathrm{E}_0\lambda^2}{1+\lambda^2} + (\mathrm{E}_1 - \mathrm{E}_0)\frac{\mathrm{i}\lambda}{1+\lambda^2}\right]\frac{1+\xi+\mathrm{i}\xi}{1+2\xi+2\xi^2} \qquad (6)$$

where $\xi = \sqrt{\nu_D/2\nu}$, $\lambda = \nu_k/\nu$, $\nu_D = \mathrm{D}\left(\frac{\partial c}{\partial \Gamma}\right)^2$ and ν_k the characteristic frequencies of diffusion and interfacial kinetic process, respectively, $E_0 = \frac{d\gamma}{dln\Gamma}$ the thermodynamic Gibbs elasticity and E_1 the high frequency limit of E. Eq. 6, in case of negligible interfacial kinetic process, that is $\lambda \to +\infty$, reduces to the classical Lucassen – van den Tempel expression for diffusion-controlled adsorption [51], i.e.

$$E = E_0\frac{1+\xi+i\xi}{1+2\xi+2\xi^2} \qquad (7)$$

The analysis of the dilation viscoelasticity versus frequency provides information on the kinetic mechanisms of the adsorption of SDS at the liquid-liquid interfaces.

Eq. 6 well describes the experimental data, assuming for the Gibbs elasticity the value calculated by the two state adsorption model. The characteristic diffusion frequency found by the fitting is three order of magnitude lower than that calculated using the thermodynamic parameters given by the model, assuming a diffusion coefficient of 10^{-10} m^2/s, which is the typical order of magnitude for short chain surfactant dissolved in water. This apparent discrepancy can be explained taking into account the fact that the adsorption of ionic surfactant, in the absence of electrolytes in the solution, yields a diffuse electric double layer close to the interface which acts as an adsorption barrier. The effect of such energy barrier, $\Delta\varepsilon$, is equivalent to assume an effective value of the diffusion coefficient, $D_{eff}=D\ exp(-\Delta\varepsilon/RT)$ [52]. The best-fit values found here for ν_D correspond to an energy barrier of about three times the thermal energy of molecules in solution, which is completely acceptable in presence of adsorption of ionic surfactant.

Moreover, though the most relevant mechanisms governing the dilational behavior seems to be the diffusional exchange with the bulk solution, in the concentration range from 10^{-4} M to 10^{-3} M, a kinetic interfacial process is also detected by the viscoelasticity data (see Table I) even if the frequency range investigated is rather limited. A hypothesis for the nature of this re-organization process may come from the observation that the re-orientation model is the most appropriate for the description of the equilibrium properties of the systems and, on the other side, the region of concentration where this kinetic process is detected is that where the equilibrium adsorptions of the two orientation states are mostly distinct (see Figure 3c).

It is worth to notice that, the same analysis of the dilational viscoelasticity data, performed adopting the Frumkin model shows the not appropriateness of the model. Assuming, in fact, the Gibbs elasticity values obtained by the fitting of the Frumkin isotherm, no agreement was found between the theoretical $E(\nu)$ and the experimental data neither using the general Eq, 6 nor with the classical Lucessen- van den Tempel Eq. 7.

Thus, even if in principle the appropriate isotherm for this ionic system should consider a lateral electrostatic interaction between the adsorbed molecules, it is clear that the Frumkin model is not sufficient to describe the adsorption of this surfactants even assuming a 2D compressibility of the adsorbed layer. The role of the re-orientation of the adsorbed molecules seems in fact to be fundamental.

The most appropriate model for this system should include both the re-orientation and the lateral interaction. However, such general model would be practically useless because of

the large number of parameters. Thus, in order to estimate the interaction parameter, we applied the Frumkin isotherm separately at high and low concentration, using the two molar areas obtained by the two state model. The results provide a_F=-1.16 for both the low and high coverage zones and show that the behavior of the coverage at low surface pressure is in agreement with that obtained with the 2 states model. In particular, the value of the interaction parameter, a_F, is much smaller than that resulting from the fitting of the Frumkin isotherm on all the concentration range.

Thus, we can conclude that assuming the two states model is the most appropriate way to describe the thermodynamic and kinetic adsorption properties of this system while the electrostatic interaction plays only a marginal role. In fact, at the water/oil interface, the interaction of the molecule alkyl tails with the oil molecules prevails on the lateral electrostatic repulsion.

Drop Coalescence

The conditions for coalescence of droplets of pure dodecane immersed in SDS solutions at different concentration, 10^{-7}M, 10^{-6} M and 10^{-5}M, brought in contact at different ageing time, have been investigated using the set-up described in the methods section.

The results show that with surfactant concentration of $1\cdot10^{-6}$ M and higher, coalescence is not observed, even if the drops are forced together several times, while for $1\cdot10^{-7}$ M, coalescence events are observed for “fresh” liquid interfaces, that is immediately after the formation of the drop. For all the cases investigated, after a time of the order of a hundred seconds from the formation of the droplets, it was not possible to observe coalescence. Figure 6 shows, as paradigmatic examples of the observed behaviors, pictures from the coalescence essays. The sequence of pictures a-b illustrate the case where coalescence occurs immediately after the drop contact and the two drops merge in a single one. In the sequence c-d instead coalescence is prevented even when the drops are forced together.

It is important to notice that the correct comparison of the results of coalescence experiments with the emulsion properties requires considering the SDS concentration in the aqueous matrix of emulsions lower than the initial one, due to the adsorption of the surfactant at the liquid-liquid interface.

For these reasons, coalescence experiments have been performed also with dodecane droplets immersed in the aqueous phase of an emulsion obtained with 0.5 and 0.2 of dodecane volume fraction. However also in this case, for SDS solutions with surfactant

concentration of $1 \cdot 10^{-6}$ M and higher, coalescence is not observed and, for $1 \cdot 10^{-7}$ M, coalescence only occurs for fresh droplet surfaces.

Even if the reported study of coalescence deserves a more quantitative and statistically relevant investigation, the observed trend is qualitatively clear, showing that coalescence is already prevented at SDS concentrations well below the cmc.

Such result is coherent with the observation by other authors [53] on the stability of dodecane-water-dodecane emulsion films containing the anionic surfactant AOT, which were shown to be indefinitely stable in a wide range of surfactant and electrolyte concentration, attributing such effect to the large repulsive forces within the film. Long-term stability for spherical emulsion films of supramicellar SDS solutions in decane was also reported in ref. [54].

It is generally accepted that the effective coalescence hindering of SDS in foams and emulsions arise from the electrostatic repulsion between the surfactant layers at the two sides of the liquid film between bubbles/droplets. The results reported here suggest that for water-alkane emulsions an additional mechanism may help the stabilization. In fact, as show in Figure 2, the possibility for the surfactant molecules to reorient provides a large coverage already at a SDS concentration of $1 \cdot 10^{-5}$M, when the effect on surface tension is a decrease of just a few mN/m.

Emulsion properties

Emulsions were obtained according to the method described above for five different SDS concentrations, spanning from $1 \cdot 10^{-7}$ M to $7 \cdot 10^{-4}$ M. For each SDS concentration, two values of oil fraction in volume, 0.2 and 0.5, were investigated.

Figures 7 and 8 show, respectively, the relative emulsion height, h_{rel}, monitored during the destabilization process and the images of the same emulsions after two hours and two months from the formation.

For Φ_d =0.2 (Figure 7a), for the lowest surfactant concentration, the aqueous and dodecane phases are completely separated within 5 minutes, while SDS solutions at $1 \cdot 10^{-6}$ M provide emulsions slightly more stable where the relative height h_{rel} reaches a constant value of about 0.2, after 10 minutes. In this case, however, a non-emulsified fraction of dodecane remains above the emulsion for all the time, since immediately after the emulsification. For all the higher surfactant concentrations, from $1 \cdot 10^{-5}$ to $7 \cdot 10^{-4}$ M, after a

time which depends on the concentration, h_{rel} reaches a value of about 0.3 and remains constant for more than two months. The dodecane phase in these cases is always completely emulsified.

A similar behavior has been observed for Φ_d=0.5 (Figure 7b). For SDS concentration of $1\cdot10^{-7}$M and $1\cdot10^{-6}$ M, the complete separation of the emulsions into two phases is attained in 5 minutes and 8 hours, respectively. In the second case, however, h_{rel} is already lower than 0.1, after 10 minutes. The situation changes for the higher surfactant concentrations, which provide rather stable emulsions. In fact, at the beginning the emulsions occupy the whole liquid phase, then, after a continuous decrease of h_{rel}, for a time of the order of 100 minutes, the emulsions reach a stationary state with a constant value of h_{rel}, weakly dependent on the surfactant concentration.

Moreover, it is worth to mention that, while for the SDS concentration of $7\cdot10^{-5}$ M and $7\cdot10^{-4}$ M, the dodecane phase remains completely emulsified, at least for 2 months (see Figure 8), this is not true for c=$1\cdot10^{-5}$ M where a fraction of dodecane appears above the emulsion just after one minute from the formation.

Thus we can conclude that it is possible to obtain a good stability of emulsion for both the values of Φ_d investigated and SDS concentration in the range $1\cdot10^{-5}$M – $7\cdot10^{-4}$ M, even if in the case of $1\cdot10^{-5}$ M, for Φ_d=0.5, the dodecane phase is not completely emulsified (figure 8).

The evolution of the average droplet radii during 3 weeks of the Φ_d=0.5 emulsions with different SDS concentration measured by optical microscopy are reported in Figure 9. The microscopy images were acquired from the side of the cell at a depth of 10 mm from the top of the emulsion. In Figure 9b examples of images used for the evaluation of the average radius are reported. In order to warrant a statistically adequate number of droplets, each point in Figure 9a has been obtained by the analysis of at least 20 images, mapping a horizontal strip at the given depth.

It is apparent from the figure that the droplet sizes do not vary appreciably after the initial transient. After 2 weeks the average radii in the emulsions with SDS concentrations $1\cdot10^{-5}$ M, $7\cdot10^{-5}$ M and $7\cdot10^{-4}$ M are respectively 11.5 μm, 10.1 μm and 9.8 μm.

For the same emulsion formulations and Φ_d= 0.5, the time evolution of the droplet size distribution has been investigated also by DLS.

Figure 10 reports the evolution of the average drop radius, R_d, corresponding to the maximum of the droplet size distributions in number obtained by DLS. The bars are the width at half height of the distribution, which provides an estimation of the emulsion polydispersity.

According to the method described in previous section, each R_d value reported in Figure 10 has been obtained on a sample extracted from the emulsion while it is evolving in time, that is to a given age of the total emulsion.

It is important to underline that the buoyancy effects due to the density difference between water and dodecane actually limit the range of size detectable by DLS analysis. In fact, during the DLS essays, before reaching the stationary regime, necessary to acquire appropriate correlation functions, that is purely Brownian motion of the droplets, a transitory phase was observed, presumably related to the buoyancy that has the effect of selectively removing from the DLS acquisition zone the larger droplets, i.e. those bigger than few microns. Standing the above considerations, the DLS essays are not quantitatively representative of the evolution of the whole droplet size distribution in the investigated emulsion. Despite this limitation, the results by DLS analysis can be utilized to get insights into the processes involved in the emulsion evolution.

The average radius for the emulsion with SDS concentration of $7 \cdot 10^{-4}$ M shows, in fact. a definite increasing trend with time. Since, as shown in previous section, coalescence is strongly hindered, Ostwald Ripening (OR) remains the only process that could contribute to the emulsion evolution after the transient stage.

For SDS concentration of $7 \cdot 10^{-4}$ M, Figure 11 evidences that a linear dependence exists between R_d and $t^{1/3}$, corresponding to a linear increase of the average drop volume. This is the characteristic signature for the Ostwald ripening process [55], associated to a variation of the average radius given by

$$\frac{4}{3}\pi(R_d^3 - R_{d0}^3) = \Omega\, t \qquad (8)$$

where the volume rate Ω depends on the interfacial tension and on other characteristics of the two liquid phases such as the solubility and the diffusion coefficient. Though this value may differ of orders of magnitude passing from the most simplified conditions of very

diluted emulsions to concentrated ones, where the effect of droplets proximity becomes important [13], the linear dependence on time is preserved.

From the best fit slope of the data in Figure 11 we obtain Ω=3.2 10^{-8} $\mu m^3/s$, which is in reasonable agreement with those previously reported in ref. [14] ($1.1 \cdot 10^{-7}$ $\mu m^3/s$), for a dodecane-in-water emulsions stabilized by SDS in absence of electrolytes. The latter data refers, in fact, to a semidilute (5% wt) emulsion stabilized by SDS at a concentration above cmc. The smaller value of Ω obtained here in spite of the larger volume ratio, can be attributed to the lack of micellar solubilization, which may be not sufficiently compensated by the rate increase due to the transport across the films between the droplets [56, 57].

It is worth to notice that for SDS concentration of $7 \cdot 10^{-4}$ M, according to the Gibbs criterion, one can assert that the OR process is not arrested by the presence of adsorbed layer, at difference with the intermediate concentration of $7 \cdot 10^{-5}$ M (see Figure 3b).

On the other side, assuming the value obtained here for the rate Ω, the increase of the average drop volume over the timescale of the present investigation (20000 min) is of the order of 0.15 μm^3, which corresponds to a variation of less than 20 nm on 1 μm radius. Therefore, standing the limitation of the DLS method, such tiny increase cannot be appreciated in population of droplets of micrometric size. This is in fact the case of the emulsions stabilized by the lowest SDS concentration of $1 \cdot 10^{-5}$ M (Figure 10), for which the Gibbs criterion predicts again the occurring of OR.

Electrical conductivity

The depletion effect of the aqueous phase of the emulsions, due to the SDS adsorption onto the emulsion droplets interface is here quantitatively evaluated by electrical conductivity measurements, according to the method described in previous section.

For these measurements, the aqueous phases were spilled from the emulsions after the achievement of the stationary condition of the emulsified layer that is about 4 days since the emulsification.

Figure 12 shows the measured conductivities of aqueous solutions, providing the master curve to access the SDS concentration. The values obtained for the aqueous matrix phase sampled from the emulsions are also reported in the figure at the abscissa corresponding to the initial SDS concentrations in water, before emulsification. For both the emulsion volume ratios, these values lye significantly below the master curve. This is a clear

evidence of the depletion resulting from the SDS adsorption at the large droplet interface available in the emulsion. The actual SDS concentrations in the depleted emulsion matrix, after emulsification, estimated by comparing these conductivities with the master curve, are reported in Table III as c*. The values for initial concentration of 10^{-6} M are not given as, for such low SDS concentration, the electrical conductivity is of the order of the sensitivity of the instrument.

A trivial mass balance of the partition of the surfactant molecules between the bulk and the interface allows the total interfacial area, A_d, of the dodecane droplet dispersed in the emulsion to be estimated as

$$A_d = \frac{(C_{in} - C^*)}{\Gamma^*} V_w \qquad (9)$$

where Γ^* is the adsorption corresponding to the actual SDS concentration. Assuming an equilibrium relation between the adsorption and the surfactant concentration in the solution, Γ^* can be calculated through the two-state adsorption isotherm discussed above. In the case of total emulsification of the dodecane phase, Eq. 9 provides the droplet radius assuming a monodisperse droplet distribution, that is

$$R_d = \frac{3\Gamma^*}{(C_{in} - C^*)} \frac{V_d}{V_w} \qquad (10)$$

The values obtained for R_d and the total droplet area, normalized by the total dodecane volume, identified as $\sigma = A_d/V_d$, are also reported in Table III.

The value of σ for a given volume ratio increases with the surfactant concentration, which corresponds to a decrease of the average droplet radius.

The interfacial coverage θ*, corresponding to the actual SDS concentration in the aqueous emulsion matrix is also reported in the table. It is particularly significant that at given initial concentration, the values of θ are large and nearly the same for both volume ratios. This large surface coverage can be a further mechanism at the origin of the emulsion stability, as already discussed in relation to the coalescence results. Back to the physical picture of the two-state model, this is a remarkable feature resulting from the ability of the surfactant

molecules to adsorb covering a large area of the interface even with a limited amount of molecules.

These results show that independently on the initial surfactant concentration and volume ratios, for the studied conditions, the stable emulsions present similar interfacial coverage, even if they differ for the amount of area created, that is, on the amount and the size of droplets produced in the emulsion.

General Discussion

It is interesting to compare the values of the radius R_d, obtained by conductivity measurements (see Table III) with the average radii provided by microscopy observation, reported in Figure 9. In fact, for emulsions formulated with SDS concentration larger than $1 \cdot 10^{-5}$ M, the radii by conductometry are of the same order of magnitude of those by microscopy. For the lowest SDS concentration ($1 \cdot 10^{-5}$ M), instead, conductometry provides values which are one order of magnitude larger than microscopy. In this case, however, the measured conductivity lays close to the lower limit of the instrument range, so that it is affected by a large relative error. Furthermore, one must consider that R_d is calculated by σ which contains the contribution of all dodecane droplets. On the contrary, for the microscope observation, due to creaming, a significant number of big droplets is expected to transfer towards the emulsion/air interface, out of the acquisition zone. This means that microscopy tends to underestimate the average radii of droplets in the emulsions.

The analysis of the size evolution of the small droplets obtained by DLS analysis allowed us to complete the scenario and recognize the role of Ostwald Ripening in the evolution of the emulsions.

The transient observed at the initial stage of the emulsion evolution (see Figs 7) is most probably due to creaming. Its duration is, in fact, compatible with the rise of droplets with radii of the order of tens of microns over the size of the cuvette (1-2 cm), when considering concentrated emulsions [58].

Therefore, the overall results are coherent with a scenario where the main process governing the emulsion evolution, besides creaming, is the increase of the droplet size driven by the Ostwald ripening. On the contrary, the drop-drop coalescence cannot be

assumed as governing mechanism, because, as observed in the above reported coalescence experiments, it is sufficient a very small amount of SDS to avoid it.

The outstanding capability of SDS to prevent coalescence even at very low concentration seems to be in contradiction with the fact that stable emulsions cannot be obtained for SDS concentrations of $1 \cdot 10^{-6}$ M and lower. Moreover, the conductivity measurements show that the depletion of the SDS in the matrix cannot explain such contradiction.

Nevertheless, the fact that at low SDS concentration the emulsion destabilizes in a time shorter than that needed to achieve a stable emulsion layer at the larger concentrations can be explained taking into consideration the dynamic conditions of the droplets at the early stage after the emulsification. In fact, due to the small amount of surfactant, during the emulsification, relatively large dodecane droplets are produced that are subjected to a quick creaming toward the top of the cell. Destabilization may then occur by the coalescence of such drops, also with the floating planar film of dodecane that is formed at the top of the cell. In fact, compared to the conditions of the coalescence experiment described here, the conditions under which the above droplets interact each other and with the dodecane upper layer are definitely more dynamic. This implies inhomogeneous distribution of surfactant on the drop surface. In this case, at SDS concentration below $1 \cdot 10^{-5}$ M, the combination of high mobility of the adsorption layer with droplet motion [59] and collision [60] may give rise to significant coverage inhomogeneities along the droplet surface, which, not properly compensated by Marangoni flows, increase substantially the coalescence.

Summary and conclusions

We report a study of different properties involved with dodecane-in-water emulsions stabilized by SDS. The analysis of these complementary results allows us to infer some general conclusions about the behavior of these emulsions and the relation with the adsorption properties of the stabilizer.

The first macroscopical observation of the emulsions behavior have shown that high stability is obtained already at relatively low SDS concentrations, around $1 \cdot 10^{-5}$ M, while, at lower concentration the emulsions destabilize in few minutes.

The information on the time dependence of the droplets size, obtained combining the results of the different techniques, DLS, electrical conductivity and microscopy, allowed us

to get insights into the processes involved in the emulsion evolution. In particular, it was possible to conclude that drop coalescence is not relevant for the emulsions evolution, except for the very low concentration during the early stage, just after the emulsification, when drops are big and under very dynamic conditions. On the contrary the results suggest that Ostwald ripening is responsible for the emulsion evolution on long-time scale.

Moreover, the conductivity measurements show that all the stable emulsions are characterized by large and similar values of the surfactant surface coverage of the droplets. Thus, the available amount of surfactant controls the maximum area achievable in the stable emulsions and, being the volume of the disperse phase fixed, the average size of the droplets.

The variability in the estimation of the droplet size obtained with the different techniques, has been rationalized on the basis of considerations on the limitations of the different utilized methodologies and of the buoyancy effects. However, this is in any case a source of uncertainty for this type of studies, which could be avoided by using less invasive methodologies. To this aim, and to suppress the effects of buoyancy, further studies may benefit by microgravity experiments based on Diffusing-Wave Spectroscopy, performed directly on the concentrate emulsion.

Concerning the role of the SDS adsorption properties, the investigation of the interfacial properties has been fundamental to get insights into the adsorption properties of SDS at dodecane-water interface and to understand the behavior of the corresponding emulsions. In fact, the interfacial tension and dilational viscoelasticity measurements show a remarkable feature of the surfactant molecules – captured by the two-state adsorption model -, which are able to cover a large area of the interface, even with a limited amount of adsorbed molecules. Together with a high electrostatic repulsion characteristic of ionic surfactants, this feature results in a high stability of the liquid film between droplets, hindering of the coalescence.

Such conclusions rise the question, which will be the subject of further studies, if other surfactants sharing similar features are also good emulsion stabilisers.

Acknowledgements

This research was supported by the European Space Agency MAP projects “Soft Matter Dynamics”, “Particle Stabilized Emulsions -PASTA’’, and by the corresponding grant of the Italian Space Agency (contract ASI n. 2013-028-R.O.

References

1 Becher, P. *Encyclopedia of Emulsion Technology*, Marcel Dekker-New York, 1985.

2 Sadurni, N.; Solans, C.; García-Celma, M. N. Studies on the formation of O/W nano-emulsions, by low-energy emulsification methods suitable for pharmaceutical applications. *Eur. J. Pharm. Sci.*, **2005**, *26,* 438-445.

3 Wang, L. J.; Dong, J.; Chen, J.; Li, X. Design and optimization of a new self-nanoemulsifying drug delivery system. *J. Colloid Interface Sci.,* **2009**, *330*, 443-448.

4 Wang, L. J.; Li, X.; Zhang, G.; Dong, J.; Eastoe, J. Oil-in-water nanoemulsions for pesticide formulations. *J. Colloid Interface Sci*, **2007**, *314*, 230-235.

5 Sonneville-Aubrun, O.; Simonnet, J. T.; L'Alloret, F. Nanoemulsions: a new vehicle for skincare products. *Adv. Colloid Interface Sci.*, **2004**, *108*, 145-149.

6 Taisne, L.; Walstra, P.; Cabane, B. Transfer of Oil between Emulsion Droplets. *J. Colloid Interface Sci.,* **1996**, *184*, 378-390.

7 Ivanov, I.B.; Kralchevsky, P. A. Stability of emulsions under equilibrium and dynamic conditions. *Colloids Surf., A,* **1997**, *128*, 155-175.

8 Langevin, D. Influence of interfacial rheology on foam and emulsion properties. *Adv. Colloid Interface Sci.*, **2000**, *88,* 209-222.

9 Santini, E.; Ravera, F.; Ferrari, M.; Alfè, M.; Ciajolo, A.; Liggieri, L. Interfacial properties of carbon particulate-laden liquid interfaces and stability of related foams and emulsions. *Colloids Surf., A,* **2010**, *365*, 189–198.

10 Yarranton, H. W.; Urrutia, P.; Sztukowski, D. M. Effect of interfacial rheology on model emulsion coalescence: II. Emulsion coalescence. *J. Colloid Interface Sci.*, **2007**, *310*, 253-259.

11 Leal-Calderon, F. ; Schmitt, V.; Bibette, J. *Emulsion Science, Basic Principles* , Springer, **2007**.

12 Binks, B.P. *Modern Aspects of Emulsion Science*, The Royal Society of Chemistry, **1998.**

13 Schmitt, V.; Cattelet, C.; Leal-Calderon, F. Coarsening of Alkane-in-Water Emulsions Stabilized by Nonionic Poly(oxyethylene) Surfactants: The Role of Molecular Permeation and Coalescence. *Langmuir,* **2004**, *20,* 46-52

14 Weiss, J.; Herrmann, N.; McClements, D. J. Ostwald Ripening of Hydrocarbon Emulsion Droplets in Surfactant Solutions. *Langmuir*, **1999**, *15*, 6652-6657.

15 Georgieva, D.; Schmitt, V.; Leal-Calderon, F., Langevin, D. On the Possible Role of Surface Elasticity in Emulsion Stability. *Langmuir*, **2009**, *25*, 5565–5573.

16 Gibbs, J. W. *The Scientific Papers of J. Willard Gibbs*, Oxbow Press, Woodridge **1993**

17 Boos, J.; Preisig, N.; Stubenrauch, C. Dilational surface rheology studies of n-dodecyl-β-d-maltoside, hexaoxyethylene dodecyl ether, and their 1:1 mixture. *Adv. Colloid Interface Sci.,* **2013**, *197–198*, 108–117.

18 Sonin, A. A.; Bonfillon, A.; Langevin, D. Role of surface elasticity in the drainage of soap films. *Phys. Rev. Lett.*, 1993, **71**, 2342-2345.

19 Kovalchuk, V. I.; Krägel, J.; Makievski, A. V.; Ravera, F.; Liggieri, L.; Loglio, G.; Fainerman, V. B.; Miller, R. Rheological surface properties of C12DMPO solution as obtained from amplitude- and phase-frequency characteristics of an oscillating bubble system. *J. Colloid Interface Sci*., **2004**, *280*, 498–505.

20 Deminière, B.; Colin, A.; Leal Calderon, F.; Bibette, J. Coarsening due to coalescence and life-time of concentrated emulsions. *Comptes Rendus de l'Académie des Sciences - Series IIC - Chemistry*, **1998**, *1,* 163-165.

21 Bonfillon, A.; Langevin, D. Viscoelasticity of monolayers at oil-water interfaces. *Langmuir*, **1993**, *9*, 2172-2177.

22 Deshiikan, S. R.; Bush, D.; Eschenazi, E.; Papadopoulos, K. D. SDS, Brij58 and CTAB at the dodecane-water interface. *Colloids Surf., A,* **1999**, *136*, 133-150.

23 Goloub, T.; Pugh, R. J. The role of the surfactant head group in the emulsification process: Single surfactant systems. *J. Colloid Interface Sci.*, **2003**, *257*, 337-343.

24 Sole, I.; Solans, C.; Maestro, A.; González, C.; Gutiérrez, J. M. Study of nano-emulsion formation by dilution of microemulsions. *J. Colloid Interface Sci.*, **2012**, *376*, 133-139.

25 Siddiqui, S. W. The effect of oils, low molecular weight emulsifiers and hydrodynamics on oil-in-water emulsification in confined impinging jet mixer. *Colloids Surf., A,*, **2014**, *443*, 8-18.

26 Javadi, A.; Mucic, N.; Vollhardt, D. ; Fainerman, V. B.; Miller, R. Effects of dodecanol on the adsorption kinetics of SDS at the water–hexane interface. *J. Colloid Interface Sci.*, **2010,** *351*, 537-541.

27 Fainerman, V. B.; Lylyk, S. V.; Aksenenko, E. V.; Petkov, J. T.; Yorke, J.; Miller, R. Surface tension isotherms, adsorption dynamics and dilational visco-elasticity of sodium dodecyl sulphate solutions. *Colloids Surf., A,* **2010**, *354*, 8-15.

28 Boos, J.; Drenckhan, W.; Stubenrauch, C. On How Surfactant Depletion during Foam Generation Influences Foam Properties. *Langmuir*, **2012,** *28*, 9303-9310.

29 Tcholakova, S.; Denkov, N. D.; Danner, T. Role of Surfactant Type and Concentration for the Mean Drop Size during Emulsification in Turbulent Flow. *Langmuir*, **2004**, *20*, 7444-7458.

30 Tcholakova, S.; Denkov, N. D.; Lips, A. Comparison of solid particles, globular proteins and surfactants as emulsifiers. *Phys. Chem. Chem. Phys.*, **2008,** *10*, 1608-1627.

31 Loglio, G.; Pandolfini, P.; Miller, R.; Makievski, A. V.; Ravera, F.; Ferrari, M.; Liggieri, L. *Novel Methods to Study Interfacial Layers*', D. Mobius, R. Miller (eds.), Elsevier, Amsterdam, **2001**, 439–483.

32 Loglio, G.; Pandolfini, P.; Liggieri, L.; Makievski, A. V.; Ravera, F. *Bubble and Drops Interfaces*, R. Miller and L. Liggieri (Eds.), Brill, Leiden-The Netherlands, **2011**, 7-38.

33 Martinez, V. A.; Thijssen, J. H.; Zontone, F.; van Megen, W.; Bryant, G. Dynamics of hard sphere suspensions using dynamic light scattering and X-ray photon correlation spectroscopy: Dynamics and scaling of the intermediate scattering function. *J. Chem. Phys.,* **2011,** *134,* 054505.

34 Provencher, S.W. CONTIN: A general purpose constrained regularization program for inverting noisy linear algebraic and integral equations. *Computer Physics Communications*, **1982**, *27*, 229-242.

35 Cookey, G. A.; Nwokobia, F. U. Conductivity Studies of Binary Mixtures of Ionic and Non-ionic Surfactants at different Temperatures and Concentrations. *J. Appl. Sci. Environ. Manage*, **2014**, *18*, 530-534.

36 Kolev, V. L.; Danov, K. D.; Kralchevsky, P. A.; Broze, G.; Mehretea, A. Comparison of the van der Waals and Frumkin adsorption isotherms for sodium dodecyl sulfate at various salt concentrations. *Langmuir,* **2002**, *18*, 9106-9109.

37 Prosser, A. J.; Franses, E. I.; Adsorption and surface tension of ionic surfactants at the air–water interface: review and evaluation of equilibrium models. Colloids Surf., A, 2001, 178, 1–40.

38 Pradines, V.; Fainerman, V. B.; Aksenenko, E. V.; Krägel, J.; Mucic, N.; Miller, R. Adsorption of alkyl trimethylammonium bromides at the water/air and water/hexane interfaces. *Colloids Surf., A,* **2010**, *371*, 22–28.

39 Mucic, N.; Gochev, G.; Won, J.; Ulaganathan, V.; Fauser, H.; Javadi, A.; Aksenenko, E. V.; Krägel, J.; Miller, R. Adsorption of equimolar aqueous sodium dodecyl sulphate/dodecyl trimethylammonium bromide mixtures at solution/air and solution/oil interfaces. *Colloid Polym. Sci.*, **2015**, *293,* 3099–3106.

40 Fainerman, V. B.; Miller, R.; Kovalchuk, V. I. Influence of the Two-Dimensional Compressibility on the Surface Pressure Isotherm and Dilational Elasticity of Dodecyldimethylphosphine Oxide. *J. Phys. Chem. B*, **2003**, *107*, 6119-6121.

41 de Aguiar, H. B.; de Beer, A. G. F.; Strader, M. L.; Roke, S. The Interfacial Tension of Nanoscopic Oil Droplets in Water Is Hardly Affected by SDS Surfactant. *J. Am. Chem. Soc.*, **2010,** *132***,** 2122–2123.

42 de Aguiar, H. B.; Strader, M. L.; de Beer, A. G. F.; Roke, S. Surface Structure of Sodium Dodecyl Sulfate Surfactant and Oil at the Oil-in-Water Droplet Liquid/Liquid Interface: A Manifestation of a Nonequilibrium Surface State. *J. Phys. Chem. B,* **2011**, *115*, 2970–2978

43 Sammalkorpi, M.; Karttunen, M.; Haataja, M. Structural Properties of Ionic Detergent Aggregates: A Large-Scale Molecular Dynamics Study of Sodium Dodecyl Sulfate. *J. Phys. Chem. B*, **2007**, *111*, 11722-11733

44 Kawai, T.; Kamio, H.; Kon-No, K. Infrared External Reflection Spectroscopy of Sodium Dodecyl Sulfate Monolayers at the Air−Solution Interface: Removal of Bulk-Phase Water Concentration Effects. *Langmuir* **1998**, *14*, 4964-4966

45 . Fainerman, V. B.; Miller,R.; Wustneck, R.; Makievski, A. V.; Adsorption Isotherm and Surface Tension Equation for a Surfactant with Changing Partial Molar Area. *J. Phys. Chem.*, **1996**, 100, 7669-7675

46**.** Fainerman, V. B.; Zholob, S. A.; Lucassen-Reynders, E. H.; Miller, R.; Comparison of various models describing the adsorption of surfactant molecules capable of interfacial reorientation *J. Colloid Interface Sci,* **2003,** 261, 80–83

47 Fainerman, V. B.; Aksenenko, E. V.; Mucic, N.; Javadi, A.; Miller, R. Thermodynamics of adsorption of ionic surfactants at water/alkane interfaces. *Soft Matter*, **201**4,*10*, 6873-6887.

48 ISOFIT; http://www.thomascat.info/Scientific/AdSo/AdSo.htm

49 Stubenrauch, C.; Fainerman, V. B.; Aksenenko, E. V.; Miller, R. Adsorption Behavior and Dilational Rheology of the Cationic Alkyl Trimethylammonium Bromides at the Water/Air Interface. *J. Phys. Chem. B,* **2005,** *109*, 1505-1509.

50 Ravera, F.; Ferrari, M.; Liggieri, L. Modelling of dilational visco-elasticity of adsorbed layers with multiple kinetic processes. *Colloids Surf., A,* **2006**, *282*, 210-216.

51 Liggieri, L.; Miller, R. Relaxation of surfactants adsorption layers at liquid interfaces. *Curr. Opin. Colloid Interface Sci.,* **2010**, *15*, 256–263.

52 Ravera, F.; Ferrari, M.; Liggieri, L., Adsorption and partitioning of surfactants in liquid–liquid systems. *Adv. Colloid Interface Sci.,* **2000**, *88*, 129-177.

53 Binks, B. P.; Cho, W. G.; Fletcher, P. D. I. Disjoining Pressure Isotherms for Oil−Water−Oil Emulsion Films. *Langmuir*, **1997**, *13*, 7180-7185.

54 Gabrieli, R.; Loglio, G.; Pandolfini, P.; Fabbri, A.; Simoncini, M.; Kovalchuk, V. I.; Noskov, B. A.; Makievski, A. V.; Krägel, J.; Miller, R.; Ravera, F.; Liggieri, L. Spherical cap-shaped emulsion films: thickness evaluation at the nanoscale level by the optical evanescent wave effect. *Colloids Surf., A,* **2012**, *413*, 101– 107.

55 Voorhees, P. W. The theory of Ostwald ripening. *j. Stat. Phys***1985**, *38,* 231-252.

56 Krustev, R.; Platikanov, D.; Nedyalkov, M.; Permeability of Foam Common Black Films to Gas. Part 2. *Colloids Surf., A,* **1997**, 123-124, 383.

57 Ramanathan, A.; Muller, H.-J.; Mohwald, H; Krastev, R. Foam Films as Thin Liquid Gas Separation Membranes. *ACS Appl. Mater. Interfaces*, **2011**, 3, 633–637.

58 Chanamai, R.; McClements, D. Creaming Stability of Flocculated Monodisperse Oil-in-Water Emulsions. *J. Colloid Interface Sci*, **2000**, *225,* 214–218.

59 Ulaganathan, V.; Krzan, M.; Lotfi, M.; Dukhin, S. S.; Kovalchuk, V. I.; Javadi, A.; Gunes, D. Z.; Gehin-Delval, C.; Malysa, K.; Miller, R. Influence of β-lactoglobulin and its surfactant mixtures on velocity of the rising bubbles. *Colloids Surf., A,* **2014**, *460*, 361–368

60 Malysa, K.; Krasowska, M.; Krzan, M. Influence of surface active substances on bubble motion and collision with various interfaces. *Adv. Colloid Interface Sci.*, **2005**, *114–115*, 205–225.

Table I: Best- fit parameters obtained from the two states model isotherm and the modified Frumkin isotherm

Model	ω_1 (m^2/mol)	ω_2 (m^2/mol)	b (m^3/mol)	α	a_F	ε (m/mN)
Two States	$1.40\ 10^6$	$1.80\ 10^5$	2.90	2.6		
Frumkin + 2D compressibility		$5.5\ 10^5$	$5.32\ 10^{-1}$		-3.4	$9\ 10^{-3}$

Table II: Parameters obtained by fitting Eq. 6 and maintaining constant the Gibbs elasticity, E_0, at the value provided by the two state adsorption isotherm. The diffusion characteristic frequency, assuming $D=10^{-10}$ m^2/s, was ν_D=6.1 Hz for all concentrations.

C_{SDS} (M)	E_0 (mN/m)	ν_D (Hz)	E_1 (mN/m)	ν_k (Hz)
$1.0\ 10^4$	15.94	0.202	--	--
$2.0\ 10^4$	10.88	0.013	12.47	0.051
$4.0\ 10^4$	8.56	0.001	12.25	0.099
$7.0\ 10^4$	9.11	0.003	14.94	0.053
$1.0\ 10^3$	10.78	0.014	--	--

Table III: Results from the conductivity measurements on the aqueous matrix phase of emulsions. See text for the explanation of the reported quantities.

	Φ_d = 0.5				Φ_d = 0.2			
C_{ini} (M)	C* (M)	σ (m^2/L)	Θ*	R_d (μm)	C** (M)	σ (m^2/L)	Θ*	Rd (μm)
$1.0\ 10^{-5}$	$3.3\ 10^{-6}$	10.82	0.85	277.2	$5.1\ 10^{-6}$	30.50	0.88	98.4
$7.0\ 10^{-5}$	$1.8\ 10^{-5}$	72.02	0.96	41.7	$3.2\ 10^{-5}$	207.65	0.98	14.4
$1.0\ 10^{-4}$	$4.2\ 10^{-5}$	74.18	0.98	40.4	$4.5\ 10^{-5}$	283.85	0.98	10.6
$7.0\ 10^{-4}$	$4.4\ 10^{-4}$	261.56	0.98	11.5	$5.4\ 10^{-4}$	731.15	0.98	4.1

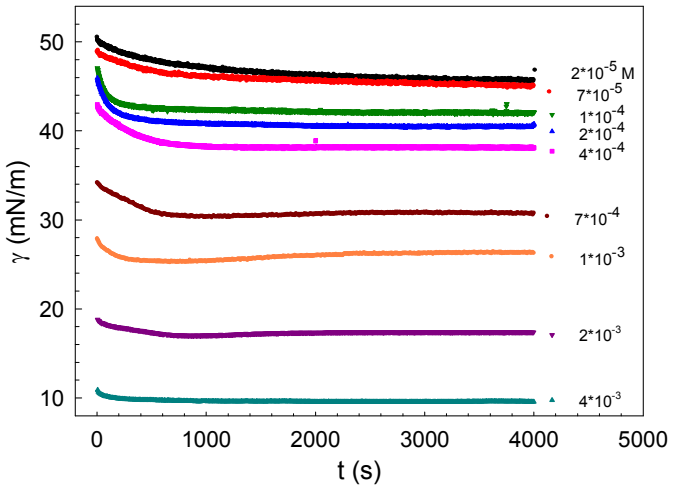

Figure 1: Interfacial tension against time of dodecane-SDS aqueous solutions for a freshly formed interface at different values of SDS concentration in water.

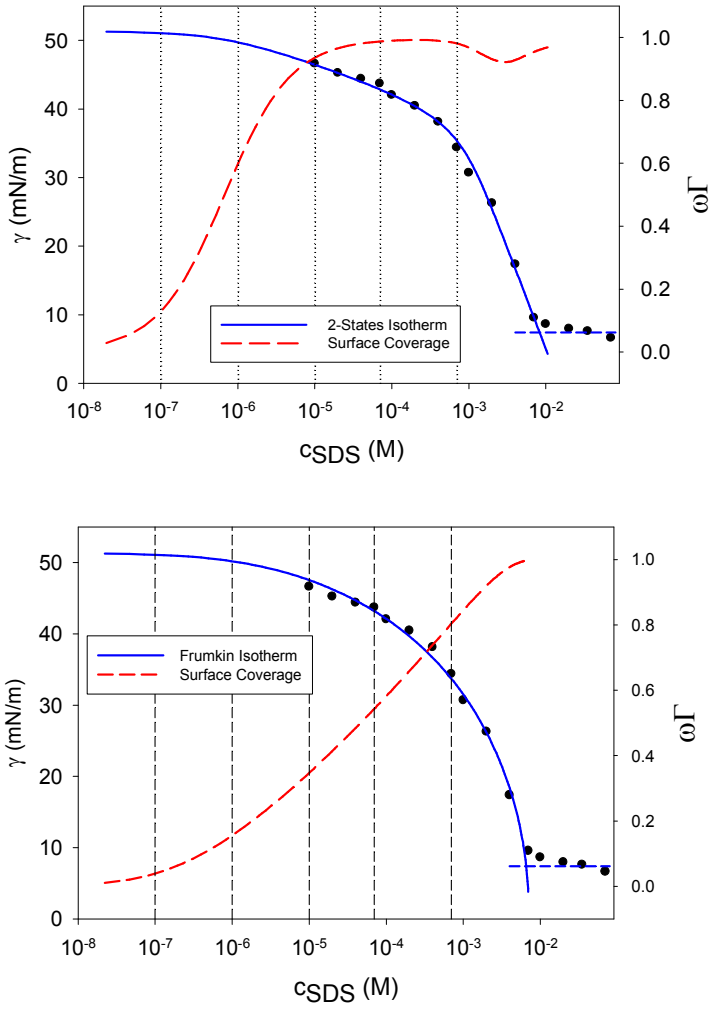

Figure 2: Equilibrium interfacial tension versus SDS concentration in water, at 20ºC, and best fit isotherms from the two states (a) and Frumkin (b) models. The surface coverage $\theta = \omega\Gamma$ is calculated by the isotherm best fit parameters. The vertical dotted lines identifies the SDS concentrations at which emulsification was investigated.

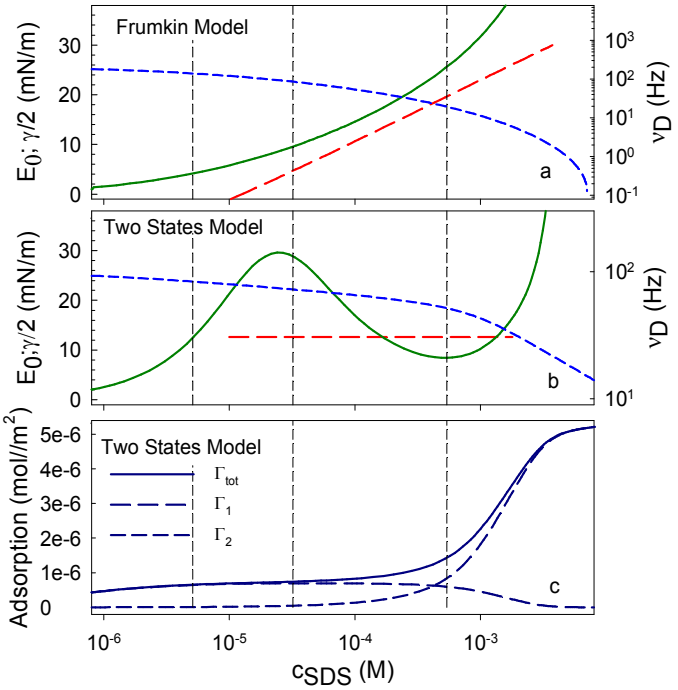

Figure 3: For the Frumkin (a) and two-states (b) models: calculated dependence on SDS concentration of: the Gibbs elasticity, E_0 (solid green curve); half the interfacial tension, $\gamma/2$ (short-dashed blue curve); characteristic frequency of the diffusion process, ν_D (long-dashed red curve), assuming $D=1\cdot10^{-10}$ m^2/s for SDS in water. Corresponding adsorptions (total, state 1 and state 2) for the two-state model (c).

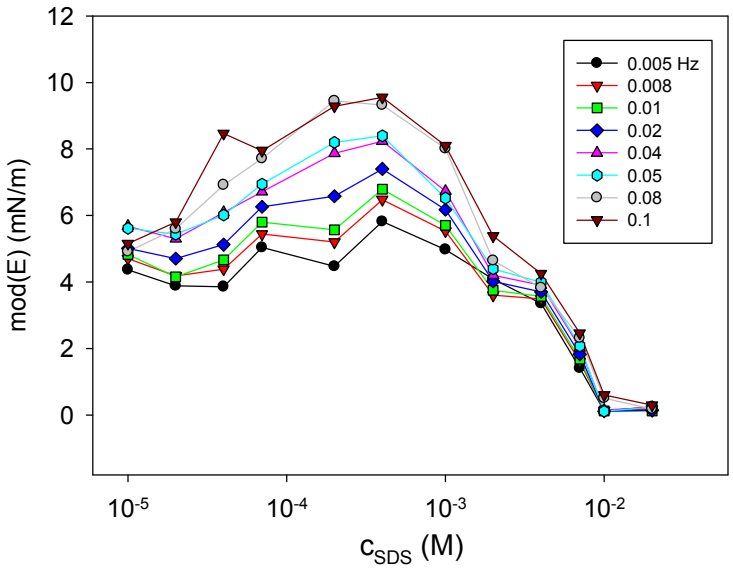

Figure 4: Modulus of the dilational viscoelasticity, E, versus the SDS concentration in water and for different values of frequency.

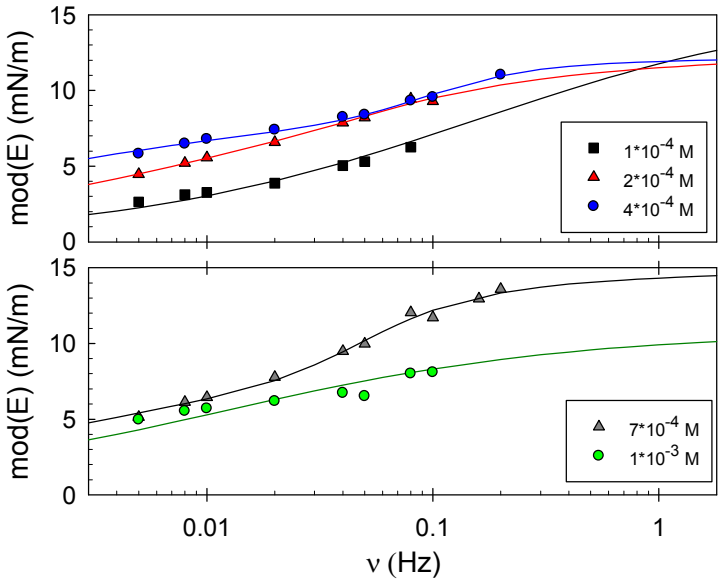

Figure 5: Modulus of the dilational viscoelasticity, E, versus frequency, for different values of SDS concentration in water, and theoretical curves obtained by fitting Eq. 6 to the experimental data. In the fitting procedure the values of the Gibbs elasticity, E_0, are fixed to those calculated for the two-state model using the best fit parameters of the adsorption isotherm (see text for details).

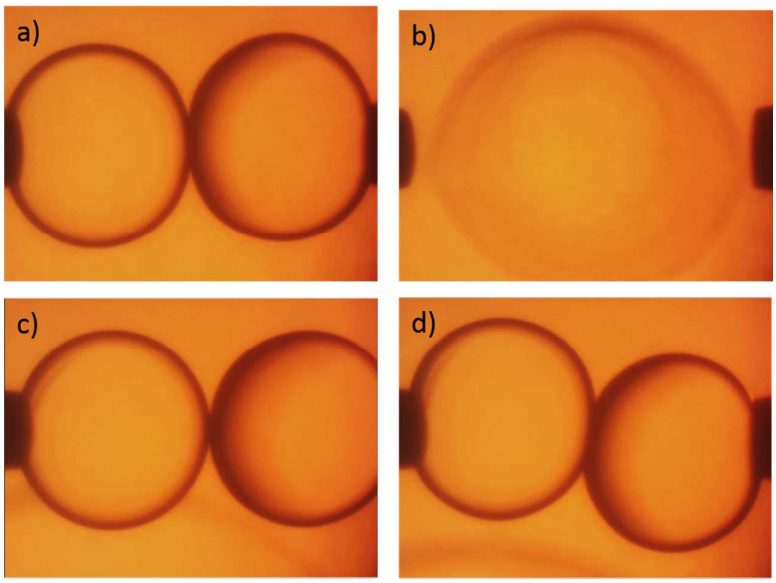

Figure 6: Examples of images from coalescence tests of dodecane droplets in SDS aqueous solution. For SDS concentration $1 \cdot 10^{-7}$ M (a,b) coalescence occurs immediately after droplets contact. For SDS concentration $1 \cdot 10^{-6}$ M (c,d) coalescence do not occurs even when forcing the droplets together.

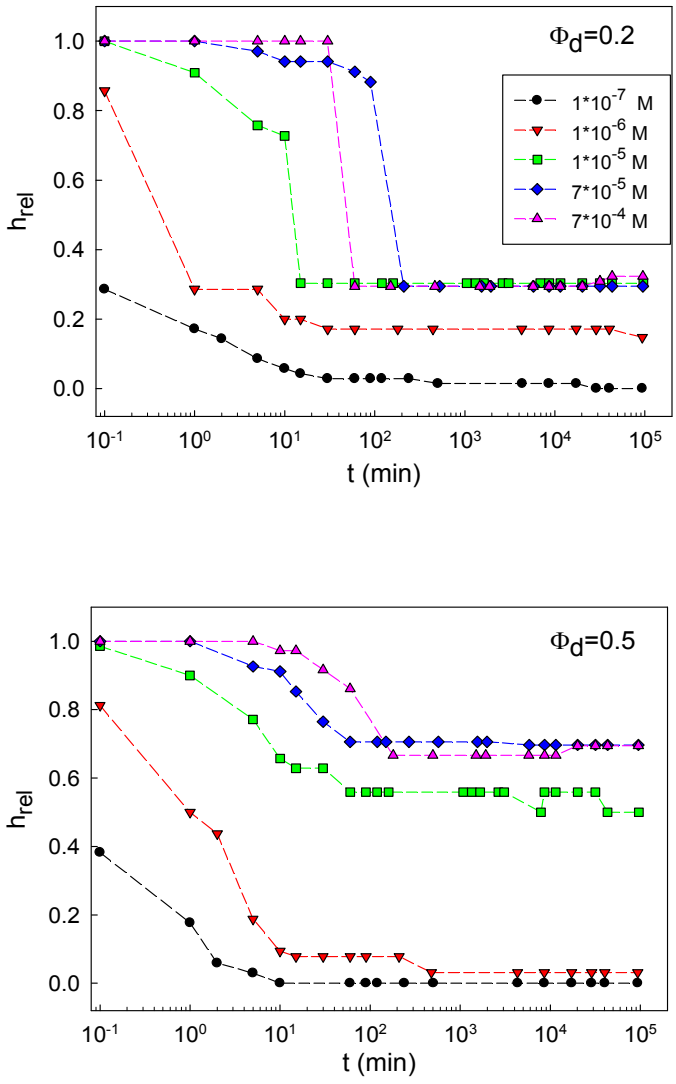

Figure 7: Relative emulsion height versus the emulsion age, for different initial SDS concentrations in water and for Φ_d=0.2 and Φ_d=0.5.

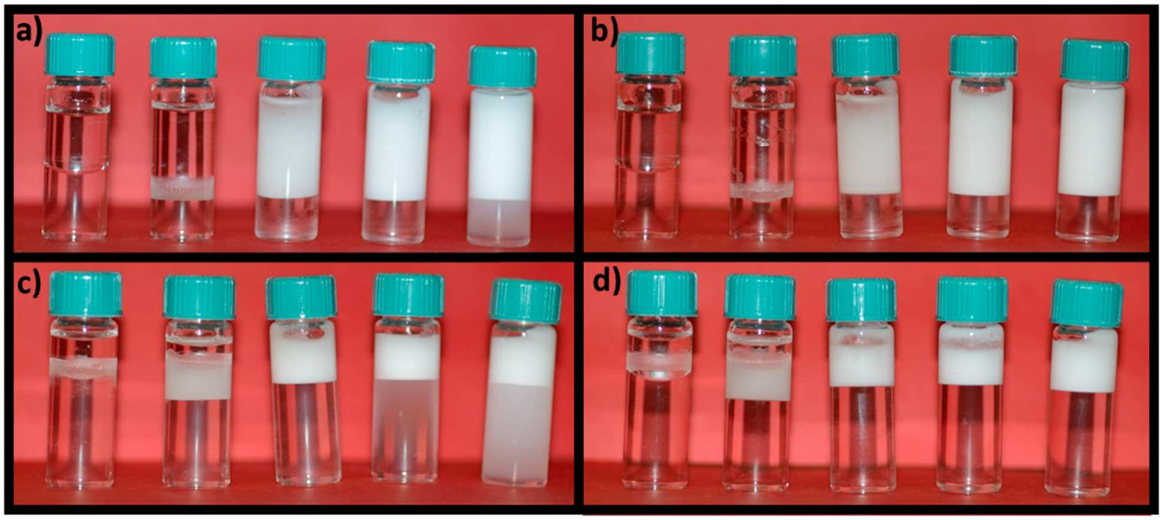

Figure 8: Emulsion images after two hours (a, c) and two months (b, d) since the formation, for Φ_d= 0.5 (a, b) and Φ_d=0.2 (c, d). In all the images the initial SDS concentration in water are from left to right: $1 \cdot 10^{-7}$, $1 \cdot 10^{-6}$, $1 \cdot 10^{-5}$, $7 \cdot 10^{-5}$ and $7 \cdot 10^{-4}$ M.

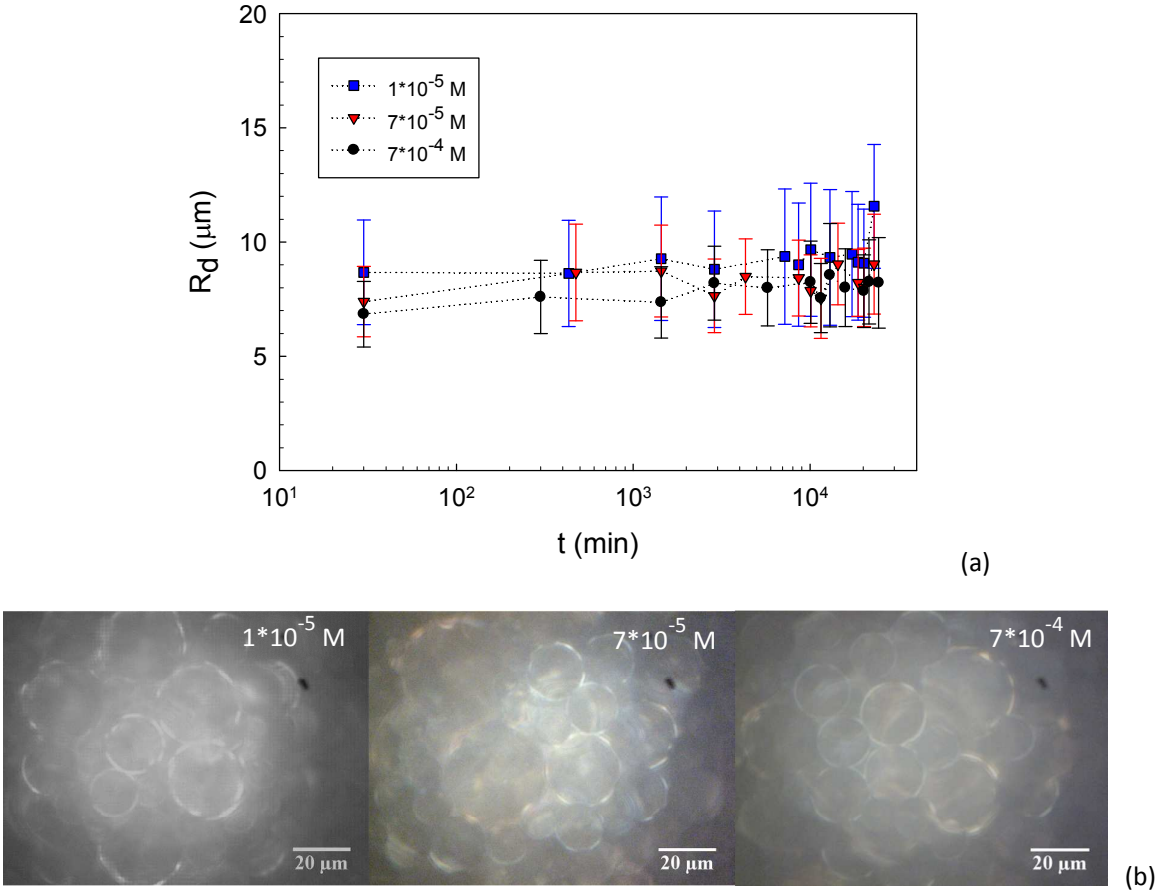

Figure 9: a) Average droplet radii by optical microscopy versus the emulsion age for different values of initial SDS concentration in water and Φ_d=0.5. The bars are the width of the size distribution. b) Examples of images utilized for the evaluation at the emulsion age of 2 weeks.

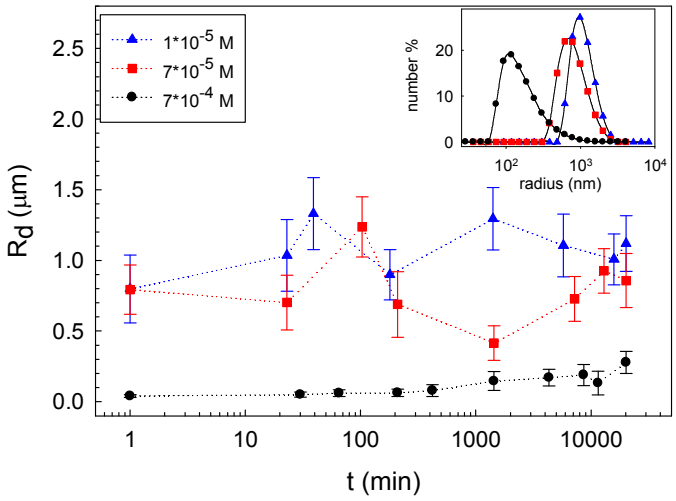

Figure 10: Average droplet radius from DLS measurements versus the emulsion age, for different values of initial SDS concentration in water and Φ_d=0.5. The bars represent the width of the distribution. The insert reports the radius distribution in number corresponding to each SDS concentration at the emulsion age of two weeks.

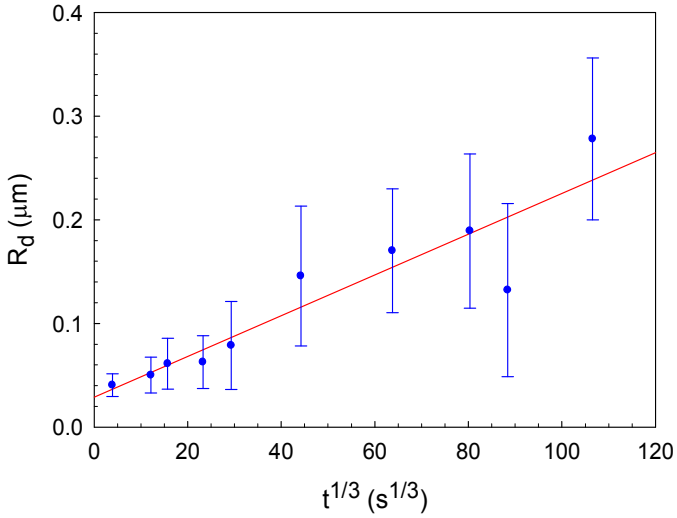

Figure 11: Same data as Figure 10, for initial SDS concentration in water of $7 \cdot 10^{-4}$ M, plotted against $t^{1/3}$, and the best fit straight line whose slope provides an Ostwald ripening rate of 3.2 10-8 µm3/s.

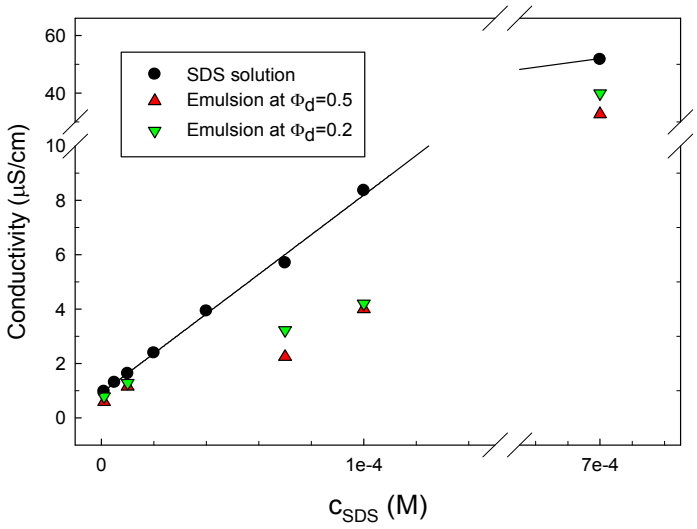

Figure 12: Electrical conductivity of aqueous SDS solutions against concentration (calibration curve) and of the emulsion aqueous phase against the initial SDS concentration at two different dodecane fractions.

Adsorption of SDS at water/dodecane interface in relation to the oil in water emulsion properties,

S. Llamas, E. Santini, L. Liggieri, F. Salerni, D. Orsi, L. Cristofolini, F. Ravera

Graphical Abstract